Articles

Electron Paramagnetic Resonance of D-Xylose Isomerase: Evidence for Metal Ion Movement Induced by Binding of Cyclic Substrates and Inhibitors†

Ralf Bogumil,‡,§ Reinhard Kappl,‖ Jürgen Hüttermann,*,‖ and Herbert Witzel‡

Institut für Biochemie, Universität Münster, Wilhelm Klemm Strasse 2, D-48149 Münster, Germany, and Fachrichtung für Biophysik und Physikalische Grundlagen der Medizin, Universität des Saarlandes, D-66421 Homburg (Saar), Germany

Received September 24, 1996; Revised Manuscript Received December 19, 1996⊗

ABSTRACT: The interactions of substrates and inhibitors with the Mn^{2+} ions in the binuclear active center of D-xylose isomerase (XylI) were investigated by EPR spectroscopy at X- and Q-band frequencies. The metal binding site 1 (A site) was specifically occupied with Mn^{2+} ions by blocking the high-affinity metal binding site 2 (B-site) either with Co^{2+} ions, resulting in a catalytically active enzyme, or with Cd^{2+} or Pb^{2+} ions yielding an inactive enzyme species. Incubation of both the Co^{2+}/Mn^{2+}- and the Cd^{2+}/Mn^{2+}-XylI with the acyclic inhibitor xylitol revealed EPR spectra with well-resolved hyperfine patterns, but with increased zero field splitting (zfs) parameter D compared to the spectra without inhibitor. D was estimated by spectral simulation of the central $-1/2 \leftrightarrow 1/2$ fine structure transition. D values of 33 and 50 mT were obtained for the Co^{2+}/Mn^{2+}-XylI and the Cd^{2+}/Mn^{2+}-XylI samples, respectively. These results indicate direct interaction of the xylitol with the Mn^{2+} in the A-site. More drastic changes are observed with the substrates D-xylose and D-glucose and with the cyclic inhibitors 5-thio-α-D-glucose and 2-desoxy-D-glucose. For Cd^{2+}/Mn^{2+}-XylI, the EPR spectra with substrates and cyclic inhibitors are similar to each other but different from the spectra with the acylic inhibitor xylitol. They exhibit well-resolved line patterns with a relative large zero field splitting, which was estimated to be in the range of $D = 65-85$ mT in the various complexes. Binding of substrates or of cyclic inhibitors to the Co^{2+}/Mn^{2+}-XylI yields EPR spectra without resolved hyperfine interactions, indicative of dipolar interaction between the two paramagnetic metal ions. This can be explained with a decrease in the metal−metal distance. Furthermore, the EPR data strongly suggest that the corresponding metal ion movement is induced by binding of the cyclic conformation of either substrates or cyclic inhibitors and not by binding of the extended form of the sugars.

D-Xylose isomerase[1] (XylI) (E.C. 5.3.1.5.) is a bacterial metal-ion activated tetrameric enzyme that catalyzes the conversion of the aldose D-xylose to the ketose D-xylulose. It also converts D-glucose to D-fructose, a reaction widely used in biotechnological processes to produce high-fructose corn syrup from starch (Verhoff et al., 1985). XylI is specific for the α-anomers of the sugar substrates (Schray & Rose, 1971).

Bacterial xylose isomerases consist of four identical subunits with molecular weights near 43 000 Da, and they have an absolute requirement for bivalent metal ions. The enzymes from *Streptomyces* are best activated by Mg^{2+}, whereas partial activity is reached with Co^{2+}, Mn^{2+}, and Fe^{2+} (Sanchez & Smiley, 1975; Callens et al., 1986; Sudfeldt et al., 1990).

The X-ray structures of xylose isomerases from different bacterial strains have been solved and were found to be very similar: *Streptomyces rubiginosus* (Carrell et al., 1984, 1989; Dauter et al., 1989, 1990; Whitlow et al., 1991), *Streptomyces olivochromogenes* (Farber et al., 1989; Lavie et al., 1994), *Athrobacter* (Henrick et al., 1989; Collyer et al., 1990), *Actinoplanes missouriensis* (Rey et al., 1988; Jenkins et al., 1992), *Clostridium thermosulfurogenes* (Meng et al., 1991). The residues, which ligate to the two metal ions and other important residues in the active site, are conserved in all species. The two metal ions, which are bridged by a glutamate residue, are separated by a distance of 490 pm in the substrate-free form. In the Mn^{2+}-substituted enzyme metal binding site 1 (or A-site) is constituted by four carboxylate groups and two water molecules. The metal binding site 2 (or B-site) has one histidine, three carboxylate groups, and a water molecule as ligands. The stereochemical arrangement of the metal sites and their nomenclature are presented in Chart 1 [according to Whitlow et al. (1991)], in which the bound water molecules are omitted for clarity.

Several structures with substrates and inhibitors have been solved. The substrates were found both in the extended-chain (Carrell et al., 1989; Collyer et al., 1990; Whitlow et al., 1991; Lavie et al., 1994; Lambeir et al., 1992) and in the cyclic form (Whitlow et al., 1991; Farber et al., 1989).

† This work was supported by grants from the Bundesministerium für Forschung und Technologie (BMFT), Grant Number 0318796 B, and from the Deutsche Forschungsgemeinschaft (DFG).

* To whom correspondence should be addressed.

‡ Universität Münster.

§ Present address: Biochemisches Institut der Universität Zürich, Winterthurer Strasse 190, 8057 Zürich, Switzerland.

‖ Universität des Saarlandes.

⊗ Abstract published in *Advance ACS Abstracts,* February 1, 1997.

[1] Abbreviations: XylI, xylose isomerase; zfs, zero field splitting.

S0006-2960(96)02406-3 CCC: $14.00

Chart 1

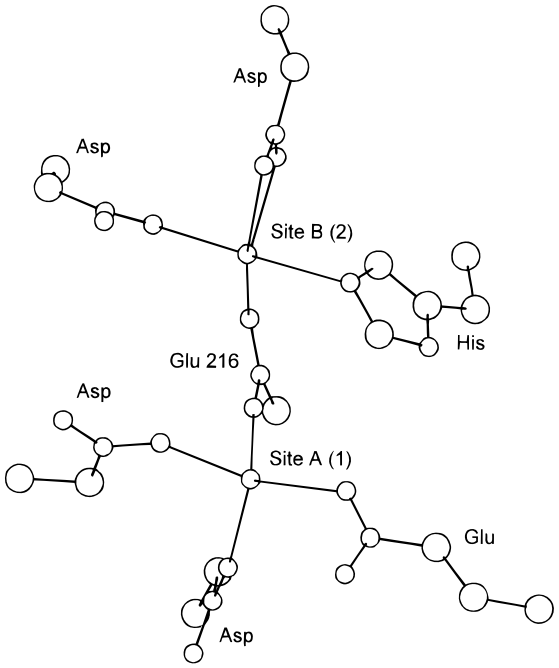

In the structures with substrate more than one position for the metal ion in site 2 is found. These results are interpreted with movement of the metal ion during substrate binding and catalysis. On the basis of the crystallographic analysis, a metal-mediated 1,2 hydride-shift mechanism was proposed for the isomerization (Collyer et al., 1990; Whitlow et al., 1991; Farber et al., 1989). It was assumed that the hydride shift should follow a ring-opening step and occur on the extended-chain form of the sugar (Collyer et al., 1990; Whitlow et al., 1991). Recently, Meng et al. (1993) proposed a different mechanism, in which the substrate molecule entering the hydride-shift step is still in the cyclic form.

The two metal binding sites can be differentiated with Co^{2+} electronic absorption and MCD spectroscopy (Callens et al., 1988; Sudfeldt et al., 1990) and with EPR, ENDOR, and electron spin echo envelope modulation spectroscopy using VO^{2+} or Mn^{2+} as paramagnetic probes (Bogumil et al., 1991, 1993; Dikanov et al., 1995). These studies have demonstrated that the B-site is the high-affinity metal binding site for the bivalent Co^{2+}, Mn^{2+}, VO^{2+}, Cd^{2+}, and Pb^{2+} cations, while trivalent ions like Eu^{3+}, Sm^{3+}, and Al^{3+} have higher affinity for the A-site. Studies on mixed-metal derivatives have shown that both binding sites must be occupied with Mg^{2+}, Co^{2+}, or Mn^{2+} cations to obtain catalytically active species. If the B-site is occupied by Cd^{2+} or Pb^{2+} and the A-site by Co^{2+} or Mn^{2+} the catalytic activity is lost, although substrates and inhibitors can still bind to the A-site (Sudfeldt et al., 1990; Bogumil et al., 1993).

The basis for the measurements presented here is our previous X- and Q-band EPR study on the two Mn^{2+}-substituted binding sites of XylI from *S. rubiginosus* (Bogumil et al., 1993). EPR spectroscopy of Mn^{2+}-substituted metalloproteins is widely used to investigate the coordination sphere of metal binding sites in metalloproteins, since the method is very sensitive to the symmetry of the ligand field of the bound Mn^{2+} (Reed & Markham, 1984). In our previous study both metal binding sites were specifically occupied by Mn^{2+} and the zero field splitting (zfs) parameters of the Mn^{2+} were determined by spectral simulation of the Q-band EPR spectra. It could be shown that the ligand sphere of the high-affinity B-site becomes less distorted upon occupation of the low-affinity A-site with Mn^{2+}. Changes in the A-site caused by different metals in the B-site were studied with help of mixed-metal derivatives, in which the B-site was specifically occupied with Co^{2+}, Cd^{2+}, and Pb^{2+} and the A-site with Mn^{2+}. In the catalytically active Co^{2+}/Mn^{2+}-XylI the Mn^{2+} in the A-site gives rise to a nearly isotropic Q-band EPR spectrum with small zero field splitting parameters. When Co^{2+} is substituted with the larger Cd^{2+} and Pb^{2+} cations, the catalytic activity is lost and significant distortions in the ligand environment of the A-site are observed as evidenced by a significant increase in the zero field splitting parameters.

In the present work the EPR spectra of the different mixed-metal derivatives in the presence of substrates and inhibitors are analyzed. To differentiate between binding of cyclic and acyclic forms of the sugars two kinds of inhibitors were used. The acyclic polyol xylitol resembles the extended form of the substrates, while in the cyclic substrate analogue 5-thio-α-D-glucose the hemiacetal conformation is stabilized by the sulfur. The results of the spectroscopic measurements in solution are compared with the different X-ray structures in the presence of substrates and inhibitors.

MATERIALS AND METHODS

D-Xylose, D-xylulose, D-glucose, D-fructose, 2-desoxy-D-glucose, and 5-thio-α-D-glucose were obtained from Sigma. The cation salts $MnCl_2$, $CdSO_4 \cdot 6H_2O$, and $Pb(CH_3COO)_2$ were purchased from Merck.

A crystalline suspension of xylose isomerase from *S. rubiginosus* was supplied by Kali-Chemie AG, Hannover, FRG. The purification of the enzyme and the preparation of the metal-substituted derivatives were described previously (Sudfeldt et al., 1990; Bogumil et al., 1993). Enzymatic activity was monitored by a continuous polarimeter test developed by Takasaki et al. (1966) and modified as described by Sudfeldt et al. (1990). Metal ions were added in stoichiometric amounts to the metal free apoenzyme. Their concentration is given in mol/mol of tetramer. The mixed-metal samples are denoted below in such a way that the occupation of the high-affinity B-site is indicated first (e.g., $4Co^{2+}/4Mn^{2+}$-enzyme). The substrates and inhibitors were added from concentrated stock solutions in 0.05 M Hepes buffer (pH 7.5) to the different metal-substituted XylI samples in the same buffer. The substrate analogues were incubated in the same way and in concentrations comparable to the mixed-metal XylI samples. Since the binding affinity of D-glucose is generally lower than for D-xylose, the final concentrations were increased compared to the measurements with D-xylose.

EPR Equipment. Samples for frozen solution EPR measurements were filled in quartz tubes (Spintec 707-SQ for X-band, 705-PQ for Q-band), immediately frozen in liquid nitrogen, and stored at 77 K. EPR measurements at X-band (9.5 GHz) were performed with Bruker ESP 300 and a Bruker ER 420 instruments, and for Q-band (34 GHz) frequencies a Bruker ER 220 instrument was used. At Q-band frequencies a variable temperature unit (gaseous nitrogen) was operated at about 100 K. The low-temperature X-band measurements were performed with a finger dewar filled with liquid nitrogen (77 K) or with an ESR 900 cryostat

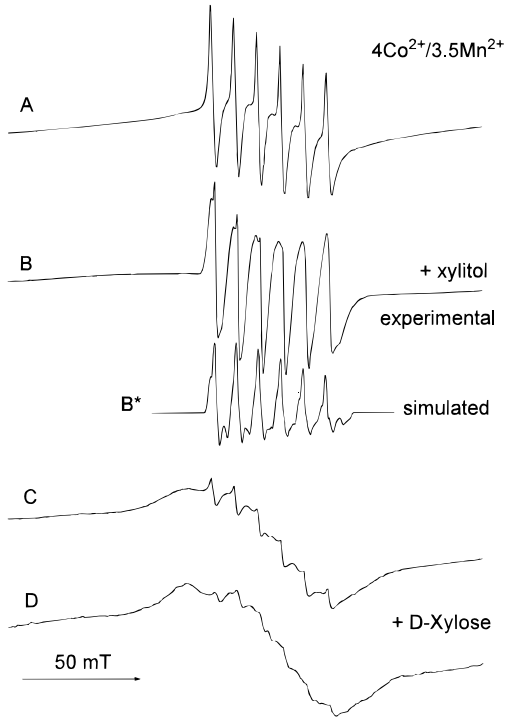

FIGURE 1: Q-band EPR spectra of $4Co^{2+}/3.5Mn^{2+}$-XylI samples at 110 K. (A) 0.68 mM $4Co^{2+}/3.5Mn^{2+}$-XylI; (B) 25 equiv of xylitol added; (C) 25 equiv of D-xylose added; (D) 250 equiv of D-xylose added. Equivalents are given in mol per mol of monomer of XylI. Trace B* is a simulated spectrum.

(Oxford Instruments) for temperatures between 4 and 60 K. The spectrometer settings for the Q-band measurements in Figures 1−5 were as follows: microwave frequency 33.5 GHz; microwave power 1 mW; modulation amplitude 0.25 mT; gain in the range 10^4-10^5. Q-band spectra simulations of the central $-^1/_2 \leftrightarrow ^1/_2$ fine structure transition were obtained with a modified version of the FORTRAN program described by Reed and Markham (1984). The presence of any unbound Mn^{2+} ions forming a typical hexaquo complex was monitored by X-band EPR measurements at room temperature in a flat cell.

RESULTS

Interactions with Acyclic Inhibitor Xylitol and Substrate D-Xylose; $4Co^{2+}/3.5Mn^{2+}$-XylI. In continuation of our work on mixed-metal samples of Mn^{2+}-substituted XylI (Bogumil et al., 1993), we have focused on the interaction of substrates and inhibitors with manganese in the A-site of the protein. The Q-band spectra of various $4Co^{2+}/3.5Mn^{2+}$-XylI samples in Figure 1 were recorded at 110 K. The top spectrum (Figure 1A) was obtained after incubation of metal-free XylI with 4 mol of Co^{2+} and 3.5 mol of Mn^{2+} per mol of tetrameric protein. It shows the expected six hyperfine lines of the naturally abundant ^{55}Mn isotope ($I = ^5/_2$) with a splitting of 9.1 mT between the maxima of the first two resonances and is characteristic of a Mn^{2+} complex with relatively small zfs parameter D. No EPR signal of the paramagnetic Co^{2+} can be detected at this temperature due to the fast relaxation of the high spin Co^{2+} ($S = ^3/_2$ state).

For the $4Co^{2+}/3.5Mn^{2+}$-XylI it was recently shown that 90% of Mn^{2+} occupy the A-site, while Co^{2+} is located in the B-site (Bogumil et al., 1993). When the inhibitor xylitol, which is a linear chain molecule, is added to the sample, a different EPR spectrum is obtained (Figure 1B). Some additional powder-type features besides the hyperfine lines become apparent in the Q-band spectrum. They are indicative for an increased zfs parameter D and a rhombic component E/D. Identical spectra were observed for xylitol concentrations between 10−25 mol per mol monomer of XylI. Systematic simulations for the $-^1/_2 \leftrightarrow ^1/_2$ transition resulted in a good agreement to the experimental spectrum concerning total spectral width and the zf-split line pattern for a value of D of 34 mT and a rhombicity of ca. $^1/_4$ (Figure 1, trace B*). In addition to an intrinsic line width of 0.7 mT a small variation in D values of 4 mT was applied to adjust to the observed line width. The D value increased considerably in comparison with the $4Co^{2+}/3.5Mn^{2+}$ without the inhibitor (12 mT, $E/D = ^1/_8$), but is still smaller than the D value of the more distorted $4Cd^{2+}/3.5Mn^{2+}$ species without inhibitor (39 mT, $E/D = ^1/_3$) (Bogumil et al., 1993). The zfs parameters are compiled in Table 1.

Table 1: Zfs Parameters of Mixed-Metal Samples of Mn^{2+}-Substituted XylI and after Addition of Inhibitor, Substrate, or Substrate Analogue

sample	simulation of central transition[a]		estimates[b]
	D (mT)	E/D	D (mT)
$4Co^{2+}/3.5Mn^{2+}$	12	$<^1/_8$	
+ xylitol	34	$^1/_4$	
+ D-xylose[c]			50−60
+ substrate analogues[c]			50−60
$4Cd^{2+}/3.5Mn^{2+}$	39	$^1/_3$	
+ xylitol	∼50	$\sim^1/_4$	
+ D-xylose			75−85
+ substrate analogues			65−85
$4Pb^{2+}/3.5Mn^{2+}$	∼54	$^1/_4$	
+ xylitol			60
+ D-xylose			75−85

[a] Simulations were performed for the $-^1/_2 \leftrightarrow ^1/_2$ transition with a modified version of the program by Reed and Markham (1984). [b] According to Reed and Ray (1971). [c] The spectra are extremely broadened.

The EPR spectrum of $4Co^{2+}/3.5Mn^{2+}$-XylI changed drastically upon addition of 25 mol of the substrate D-xylose per mol of monomer (Figure 1C). The overall spectral width increased from approximately 65 to 111 mT. The small hyperfine sextet seen in Figure 1C closely resembles the pattern of the sample without substrate (Figure 1A). To check whether it is due to a small fraction of the enzyme without bound substrate a larger excess of D-xylose (250 mol of xylose per mol of monomer) was added to the sample. In the resulting EPR spectrum shown in Figure 1D the hyperfine sextet almost completely disappeared. Since the $4Co^{2+}/3.5Mn^{2+}$ substituted enzyme is catalytically active, converting D-xylose to D-xylulose in an equilibrium reaction, samples were frozen in liquid nitrogen after a few minutes and 1, 3, or 24 h subsequently to addition of substrate. Independent from the incubation time with substrate, identical spectra to those of Figure 1C, D were observed for the corresponding concentrations of substrate. Therefore it can be excluded that non-equilibrium states contribute to the spectral pattern. Thus, the remaining hyperfine pattern for lower substrate concentration in Figure 1C can be attributed to result from Mn^{2+} in the A binding sites without substrate. Comparison of line intensities between the spectra of Figure 1A and 1C yields as a rough estimate ca. 5% of substrate-free A-sites. Higher amounts of the substrate D-xylose are needed for a quantitative binding as in the case of the inhibitor xylitol

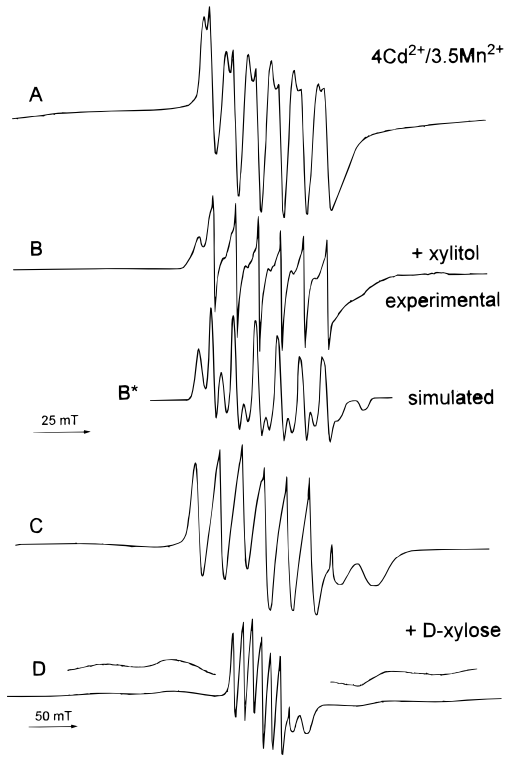

FIGURE 2: Q-band EPR spectra of $4Cd^{2+}/3.5Mn^{2+}$-XylI samples at 110 K. (A) 0.7 mM $4Cd^{2+}/3.5Mn^{2+}$-XylI; (B) 25 equiv of xylitol added; (C) 25 equiv of D-xylose added; (D) 500 mT scan of sample C, positions of outer fine structure transitions are enhanced five times. Equivalents are given in mol per mol of monomer of XylI. Trace B* is a simulated pattern.

(Figure 1B). This is in agreement with the higher affinity of the competitive inhibitor xylitol ($K_i = 0.89$ mM) compared to D-xylose ($K_m = 7.3$ mM) (van Bastelaere et al., 1991).

The spectrum of Figure 1D may be envisaged as an extremely broadened rhombic powder pattern without resolved hyperfine interaction for the central transition. There are very broad shoulders visible around field positions 1125 and 1275 mT which are related to other fine structure transitions. At X-band frequencies the spectra, besides the central transition, also exhibit zfs resonances extending from 200 mT to more than 450 mT (not shown). Control measurements at low temperatures (4 K) do not yield an improved resolution or any resolved hyperfine interactions (not shown). The EPR feature is again indicative for a large zero field splitting for which, in the absence of simulation parameters, only a rough estimate of *D* between 50 and 60 mT (Table 1) can be inferred from the field positions of the outer transitions according to the scheme suggested by Reed and Ray (1971) for axial symmetry. A nearly identical Q-band EPR spectrum is obtained by incubation of a $8Mn^{2+}$-XylI (both binding sites occupied by Mn^{2+}) with excess of D-xylose (data not shown).

Interactions with Acyclic Inhibitor Xylitol and Substrate D-Xylose; $4Cd^{2+}/3.5Mn^{2+}$-XylI. The catalytically inactive $4Cd^{2+}/3.5Mn^{2+}$-XylI without inhibitor or substrate exhibits a Q-band spectrum (Figure 2A) typical for a considerable rhombic zero field splitting. A value of 39 mT for *D* and a rhombicity of $^1/_3$ was estimated from simulation of the central $-^1/_2 \leftrightarrow ^1/_2$ transition (Bogumil et al., 1993). The line pattern is similar to that of $4Co^{2+}/3.5Mn^{2+}$-XylI with xylitol, which is characterized by a smaller zfs. In analogy, addition of xylitol to $4Cd^{2+}/3.5Mn^{2+}$-XylI induces a further increase of

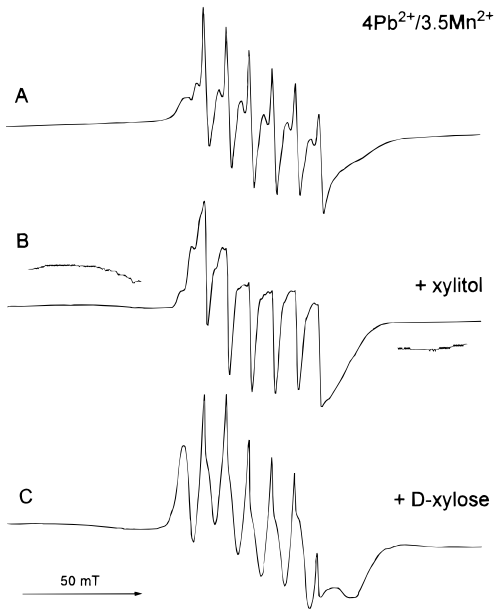

FIGURE 3: Q-band EPR spectra of $4Pb^{2+}/3.5Mn^{2+}$-XylI samples at 110 K. (A) 0.5 mM $4Pb^{2+}/3.5Mn^{2+}$-XylI; (B) 25 equiv of xylitol added, the broad outer resonances are enhanced 10 times; (C) 25 equiv of D-xylose added. Equivalents are given in mol per mol of monomer of XylI.

zfs parameters producing a well-separated low-field line and an increased overall spectral width (75 vs 84 mT) (Figure 2B). Simulation of the $-^1/_2 \leftrightarrow ^1/_2$ transition with a *D*-value around 50 mT reproduced the position of the low-field line (6.1 mT downfield of the first hyperfine resonance) and the spectral width reasonably well. However, finer details, like the pattern of forbidden transitions between the manganese hyperfine lines and line intensities, could not be obtained (Figure 2B*).

The addition of xylose to $4Cd^{2+}/3.5Mn^{2+}$-XylI samples (20 mol per mol of monomer) brings about drastic spectral changes. The overall spectral width of the $-^1/_2 \leftrightarrow ^1/_2$ transition increases to ca. 92 mT, and additional zf-split resonances are flanking the original hyperfine sextet (Figure 2C). The biphasic line shape of the low-field resonance is indicative for intermediate rhombic distortion, since in case of complete rhombicity ($E/D = ^1/_3$) typically absorptive line shapes are expected (Reed & Markham, 1984). In contrast to the $4Co^{2+}/3.5Mn^{2+}$-XylI sample with xylose, the line pattern is well resolved and does not show a pronounced broadening. The attempts to simulate the spectral pattern of the $-^1/_2 \leftrightarrow ^1/_2$ transition gave no satisfying results, which seems to be due to the involved large *D* values at or above the limits of the applicability of the used simulation routine. From an analysis of the outer zf-transitions, clearly discernible in the Q-band spectrum of Figure 2D recorded with a field scan of 500 mT, a *D* value of approximately 75−85 mT is estimated (Table 1) according to the scheme of Reed and Ray (1971).

$4Pb^{2+}/3.5Mn^{2+}$-XylI. In the absence of inhibitor or substrate the inactive Pb-substituted enzyme already shows a larger spectral width and an increased zf-splitting *D* (Figure 3A) compared to the $4Cd^{2+}/3.5Mn^{2+}$-XylI. The zfs parameter *D*, estimated from a simulation of the $-^1/_2 \leftrightarrow ^1/_2$ transition, was found to be in the range between 51 and 57 mT with an *E* value of approximately 14 mT (Bogumil et al., 1993). Again, the addition of xylitol affects a slight increase of the spectral width and changes the line pattern significantly

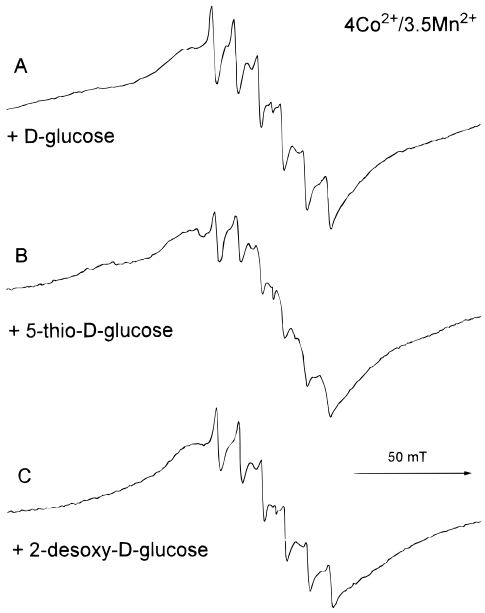

FIGURE 4: Q-band EPR spectra of 0.58 mM $4Co^{2+}/3.5Mn^{2+}$-XylI samples at 110 K. (A) 50 equiv D-glucose added; (B) 50 equiv of 5-thio-α-D-glucose added; (C) 50 equiv of 2-desoxy-D-glucose added. Equivalents are given in mol per mol of monomer of XylI.

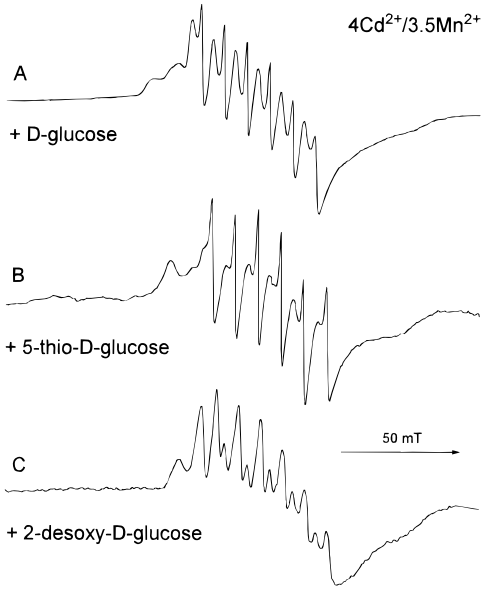

FIGURE 5: Q-band EPR spectra of 0.4 mM $4Cd^{2+}/3.5Mn^{2+}$-XylI samples at 110 K. (A) 50 equiv of D-glucose added; (B) 50 equiv of 5-thio-α-D-glucose added; (C) 50 equiv of 2-desoxy-D-glucose added. Equivalents are given in mol per mol of monomer of XylI.

(Figure 3B). Apart from the $-^1/_2 \leftrightarrow ^1/_2$ transition extremely broad lines of the other transitions are discernible at high gain around 1140 and 1275 mT, which are indicative of a *D* value around 60 mT (Table 1).

When the substrate D-xylose is added to $4Pb^{2+}/3.5Mn^{2+}$-XylI, the spectral width increases to ca. 91 mT and a well-resolved line pattern is observed (Figure 3C), similar to that seen in the $4Cd^{2+}/3.5Mn^{2+}$ D-xylose sample (Figure 2C). Hence, the effects of inhibitor and substrate on $4Pb^{2+}/3.5Mn^{2+}$-XylI are comparable (but not as pronounced) to those on $4Cd^{2+}/3.5Mn^{2+}$-XylI. However, the spectral broadening of $4Co^{2+}/3.5Mn^{2+}$-XylI with xylose (Figure 1D) is not observed for both other species.

Interactions with Cyclic Substrate Analogues. 5-Thio-α-D-glucose is an analogue of the reactive substrate anomer with the ring oxygen replaced by a sulfur. No enzymatic ketose formation is observed for this sugar (Bock et al., 1983) and competitive inhibition of D-glucose isomerization is observed with a K_i value of 33 mM (Collyer et al., 1990). In the X-ray structure of Collyer et al. (1990) the 5-thio-α-D-glucose is found in a cyclic form with C3 and C4-OH ligated to the A-site metal. The compound 2-desoxy-D-glucose is used to test the importance of the C2 hydroxyl group for the binding of the substrates. For comparison the spectra in presence of the substrates D-glucose, D-fructose, and D-xylulose were also collected. D-glucose and D-xylose have identical atomic conformations except for the presence of an additional CH_2OH group at the C-6 position in D-glucose.

$4Co^{2+}/3.5Mn^{2+}$-XylI. The spectra recorded for $4Co^{2+}/3.5Mn^{2+}$-XylI after addition of the three D-glucose derivatives are depicted in traces A−C of Figure 4. All three spectra closely resemble those after addition of D-xylose (Figure 1C,D). They are also characterized by an extreme broadening of the overall spectral width amounting up to 120 mT. On the low-field side of the $-^1/_2 \leftrightarrow ^1/_2$ transition broad features around 1130 mT are discernible, e.g., for $4Co^{2+}/3.5Mn^{2+}$-XylI with 5-thio-α-D-glucose (Figure 4B) which may arise from other electronic transitions. The hyperfine sextet pattern on top of the poorly resolved central transition presumably arises from metal sites with no glucose derivatives bound in a similar intensity as for $4Co^{2+}/3.5Mn^{2+}$-XylI with D-xylose (Figure 1C). It should be noted that the same behavior of spectral broadening is also found in the measurements with D-fructose and D-xylulose (data not shown).

$4Cd^{2+}/3.5Mn^{2+}$-XylI. In contrast to the above findings the incubation of $4Cd^{2+}/3.5Mn^{2+}$-XylI with the D-glucose derivatives results in all cases in well-resolved line patterns, which extend over a field range of approximately 100−120 mT and are indicative of a large zero field splitting. The presence of the absorptive low-field lines as well as of rather broad resonances at high field points to a pronounced rhombicity for these ternary complexes. The spectra for $4Cd^{2+}/3.5Mn^{2+}$-XylI with added glucose derivatives are presented in Figure 5A−C, which all show roughly the same overall spectral width but differ considerably in their individual line pattern. These spectral changes probably are resulting from a variation of the ratio *E*/*D* rather than of the magnitude of the zero field splitting *D*. They demonstrate the high sensitivity of Mn^{2+} EPR spectroscopy to the different modes of binding of the glucose derivatives.

The differences within this series of spectra are less significant than compared to the spectrum of $4Cd^{2+}/3.5Mn^{2+}$-XylI with xylose (Figure 2C) exposing a more axial-type spectrum. Attempts to simulate the line patterns of Figure 5 failed because of the large zfs parameters involved. From the very broad resonances barely visible in larger field scans in Q-band as well as from X-band spectra (data not shown) a rough estimate of *D* in the range 65−85 mT can be obtained according to the scheme suggested by Reed and Ray (1971).

DISCUSSION

The binding of substrates and inhibitors to the active center of xylose isomerases has been intensively studied by several groups using X-ray crystallography (Carrell et al., 1989; Farber et al., 1989; Collyer et al., 1990; Whitlow et al., 1991;

Jenkins et al., 1992; Lavie et al., 1994). In particular, the results obtained for the binding of the substrate D-xylose are not consistent. One problem is that the substrate D-xylose is in an equilibrium between the α- and β-anomer and also between the cyclic and extended form, which creates multiple binding possibilities. Furthermore, different positions of the metal ion in the B-site (or site 2) are found in several X-ray structures in presence of substrates. These results were interpreted with a movement of the metal ion in the B-site during catalysis (Collyer et al., 1990; Whitlow et al., 1991; Lavie et al., 1994).

Our EPR spectroscopic data can be best compared with the X-ray structures of Whitlow et al. (1991), since the Mn^{2+}-substituted XylI from the same species (*S. rubiginosus*) was used for the crystallographic analysis.

Binding of the Acyclic Inhibitor Xylitol. Although catalytic activity is found with Mg^{2+}, Co^{2+}, and Mn^{2+}, the coordination geometry in the A-site seems to depend on the cation. Spectroscopic studies indicate a tetrahedral or pentacoordinated Co^{2+} in the A-site (Sudfeldt et al., 1990), and X-ray crystallographic analysis revealed a tetrahedral arrangement of four carboxylate groups for Co^{2+} or Mg^{2+} in this site (Jenkins et al., 1992). In the X-ray structures of the Mn^{2+}-substituted enzyme an octahedral coordination sphere is found with two additional water molecules bound beside the four carboxylate groups (Whitlow et al., 1991). The EPR data also provide evidence for an octahedral coordination of Mn^{2+} in the A-site. The ^{55}Mn hyperfine coupling in all complexes studied is in the range of 9.1−9.5 mT, a characteristic value for octahedral Mn^{2+} complexes [e.g., Mn-$(H_2O)_6^{2+}$, $A = 9.5$ mT], whereas in tetrahedral complexes the hyperfine coupling is usually smaller (6−7 mT) (Reed & Markham, 1984). These differences between Mn^{2+} and Co^{2+} can be explained with the different properties of complex formation. The d^5 ion Mn^{2+} strongly favors an octahedral coordination sphere in aqueous solution, whereas Co^{2+} with a d^7 configuration can form relatively stable tetrahedral complexes.

The binding of xylitol creates an octahedral complex geometry for both Co^{2+} and Mn^{2+} ions. On the basis of the crystallographic analysis it has been suggested that the O2 and O4 of xylitol replace the two water ligands, resulting in a similar octahedral arrangement in the Mn^{2+} inhibitor complex (Whitlow et al., 1991).

Such a direct interaction of xylitol with Mn^{2+} in the A-site is consistent with the EPR analysis, since significant changes are observed in the EPR spectra of all xylitol complexes ($4Co^{2+}/3.5Mn^{2+}$, $4Cd^{2+}/3.5Mn^{2+}$, $4Pb^{2+}/3.5Mn^{2+}$). In all three cases an increase in the zero field splitting D was found in comparison to the spectra without xylitol. This is best seen for the $4Co^{2+}/3.5Mn^{2+}$ derivative, which shows a nearly isotropic signal without xylitol ($D = 12$ mT), whereas binding of xylitol results in an increase of D to about 34 mT. An increase in zf-splitting can be attributed to a more distorted ligand arrangement of the Mn^{2+}, although the zf-splitting is still relatively small compared to the EPR spectra with substrates. The replacement of the two water ligands with hydroxyl groups from the xylitol could explain these changes. Slight distortions of the ligand sphere of the Mn^{2+} might be expected, since the two hydroxyl groups are not as flexible as the water ligands. At present no X-ray data are available for the Cd^{2+}- and Pb^{2+}-substituted enzymes, but the same trend (increase in zf-splitting) observed in the EPR spectra indicates a similar binding of the acyclic inhibitor xylitol to these samples.

Binding of Substrates and Cyclic Substrate Analogues. The binding of the substrate D-xylose has a much stronger effect on the EPR spectral properties of the different XylI complexes. By incubation of the $4Co^{2+}/3.5Mn^{2+}$ enzyme with D-xylose an extremely broadened powder pattern is found without any resolved hyperfine interactions. Nearly identical spectral features are evident in the EPR spectra of the $4Co^{2+}/3.5Mn^{2+}$ complexes with other substrates (D-xylulose, D-glucose, D-fructose) and also in the EPR spectra with the two cyclic inhibitors 5-thio-α-D-glucose and 2-desoxy-D-glucose. The common feature of all these spectra is the unusual line broadening. We attribute the disappearance of the hyperfine interaction to the presence of dipolar interaction between Mn^{2+} in the A-site and the paramagnetic Co^{2+} or Mn^{2+} (in the case of the $8Mn^{2+}$-enzyme) in the B-site. This assignment is strongly supported by the results obtained with the samples, in which the B-site is loaded with diamagnetic Cd^{2+} or Pb^{2+} ions. In these samples incubation with substrates gives rise to significant changes in the EPR spectra, but despite of these large changes in zf-splitting, well-resolved hyperfine interactions are clearly detected.

In the substrate-free form, the two metal binding sites in XylI are 4.9 Å apart and share a common ligand (Glu 216). The analysis of the respective EPR spectra of $4Co^{2+}/3.5Mn^{2+}$ and $8Mn^{2+}$-XylI does not reveal any significant contributions of dipolar or exchange interactions between the metals in the two binding sites (Bogumil et al., 1993). The X-ray structure of Mn-substituted XylI with xylose bound reveals a reduced metal−metal distance of about 3.5 Å (Whitlow et al., 1991). It is noted, that the magnetic dipolar interaction is strongly dependent on the distance r between the dipoles ($\sim 1/r^3$) and the relative orientation of their magnetic moments (Abragam & Bleaney, 1970; Reed & Markham, 1984). With simple point dipole calculation a 3-fold increase in magnetic interaction is estimated for the observed shift of the metal in the B-site, assuming isotropic and localized magnetic moments for both metal ions. In principle, additional broadening effects can arise from reorientation of the individual anisotropic magnetic tensors of metal ions upon substrate binding, e.g., when the maximal **g** component of Co^{2+} is more closely aligned to the connecting vector between the ions. An estimate on the possible contribution of that type cannot be obtained from our spectroscopic data, since it would require the knowledge of the relative tensor orientations before and after substrate binding. However, the appearance of a very similar, extremely broadened spectrum in $8Mn^{2+}$-XylI with xylose is indicative for a dominant role of the $1/r^3$ dependence in line broadening, since for Mn^{2+} the **g** tensor is assumed to be nearly isotropic and close to the free electron value. In addition the distance dependent dipolar contribution is very sensitive to spatial disorder of the metal sites in the protein molecules, which in turn reduces spectral resolution. Attributing the spectral pattern of the complexes with substrates and cyclic inhibitors to dipolar interactions, it is postulated that the distances between the two metal ions are decreased compared to the substrate-free form.

Besides dipolar interactions, exchange interaction might also be considered. The bridging carboxylate group could in principle act as a mediator for a super-exchange pathway. Such a system is present in concanavalin A, where two metal

binding sites are 4.25 Å apart and bridged by two aspartate residues (Hardman et al., 1982). In the EPR spectra of Mn^{2+}-concanavalin A an 11-line hyperfine multiplet is found with hyperfine coupling constant A of 4.7 mT (Antanaitas et al., 1987). Such spectral properties are characteristic for exchange coupled Mn^{2+} ions with exchange coupling constant $J > A$ (Reed & Markham, 1984). However, no indications for a multiple line pattern are found in the $8Mn^{2+}$-XylI D-xylose complex even at 4 K (data not shown). Therefore it can be assumed that exchange interactions, if present at all, are rather weak in our system and the broadening can be mainly attributed to dipolar interactions. In concanavalin A one of the two bridging carboxylate groups is asymmetric (the same oxygen binds to both metal ions) and the second is a symmetric carboxylate bridge (both oxygens are involved) similar to that in XylI. The asymmetric carboxylate bridge is probably the origin of the stronger coupling found in concanavalin A. Work with different binuclear Mn^{2+} model compounds has shown that symmetric μ-carboxylate bridges result in weak antiferromagnetic coupling, whereas stronger couplings are observed in the μ-OH bridged system, where the same oxygen is bound to both metal ions (Wieghardt, 1989).

The dipolar interactions in XylI are not induced by binding of the acyclic inhibitor xylitol but are clearly evident in the spectra with the cyclic inhibitor 5-thio-α-D-glucose. The spectra of the substrates are very similar to the spectra of the cyclic inhibitor, which strongly indicates that the substrates bind in the cyclic form. This holds true for both the catalytic active and the inactive mixed-metal samples. Further support for this hypothesis comes from the measurements with the 2-desoxy-D-glucose. According to the different X-ray structures, the extended form of the substrates binds with O2 and O4 to the metal in the A-site, while in the cyclic form O3 and O4 ligate to the metal ion. The similarity of the EPR spectra of 2-desoxy-D-glucose to the spectra with substrates makes the O3 and O4 the most likely candidates for metal ion binding.

Different positions of the metal ion in the B-site were observed in several X-ray structures in presence of substrate and a metal ion movement upon substrate binding was postulated (Collyer et al., 1990; Whitlow et al., 1991; Jenkins et al., 1992; Lavie et al., 1994). The EPR study presented here gives the first direct spectroscopic evidence for such a movement. However, our results do not agree with the crystallographic analysis concerning the origin of this dynamic behavior.

On the basis of the X-ray structures it was postulated that the metal movement is following a ring opening step and is triggered by the binding of O1 and O2 of the extended form of the sugar to the B-site metal ion. During catalysis a hydroxide ion bound to this metal ion should remove the O2 hydroxyl proton of D-xylose and the negative charge on the O2 should be stabilized by the metal ion (Collyer et al., 1990; Whitlow et al., 1991; Jenkins et al., 1992). Furthermore, Lavie et al. (1994) suggested that the deprotonation of the O2 causes the shift of the metal ion in the B-site. Our spectroscopic results indicate that binding of the cyclic form of substrates or substrate analogue inhibitors is sufficient to induce the shift of the metal ion in the B-site. Thus, the metal ion movement and the isomerization reaction are two independent processes, which are not necessarily coupled as suggested by Lavie et al. (1994).

On the basis of kinetic parameters for α- and β-D-glucose of wild-type and some mutants XylI isomerases, Meng et al. (1993) proposed another model for the catalytic mechanism in which the hydride shift would occur on the cyclic form of the substrate rather than on the extended form. This model would be in much better agreement with our spectroscopic data. One problem with the model of Meng et al. (1993) is, however, that the metal ion in the B-site would not play any significant role and no metal ion shift would be necessary. However, kinetic data and metal-ion binding studies have shown that both metal binding sites must be occupied with catalytic active metal ions like Mn^{2+}, Mg^{2+}, and Co^{2+} (Sudfeldt et al., 1990; Callens et al., 1988). Clearly, further studies are necessary to resolve the mechanistic details for this enzyme.

The EPR measurements of the mixed metal samples with Cd^{2+} or Pb^{2+} in the B-site show that substrates still bind to the Mn^{2+} in the A-site, but no catalytic activity is found. The large zf-splitting in the EPR spectra of these samples with substrates indicates significant distortions of the ligand field of Mn^{2+} in the A-site. Since Cd^{2+} and Pb^{2+} are diamagnetic, it is not possible to prove by EPR if these cations also change their position upon substrate binding. It might be that the relative large distortion of the ligand field in the A-site are in fact due to constraints imposed by a shift of the metal ion in the B-site toward the A-site. Another possibility is that the inhibitory effect of these larger cations is based on the lack of the dynamic behavior, since their increased ionic radius might prevent the shift. In this case the larger distortion upon binding of the cyclic substrates and inhibitors compared to the xylitol could be due to the binding of the O3 and O4 hydroxyl group of the substrates, which do not have as much conformational freedom in the cyclic form as the O2 and O4 hydroxyl groups of the extended polyol xylitol.

ACKNOWLEDGMENT

While this paper was being reviewed, Professor Herbert Witzel died at the age of 72. We wish to dedicate the paper to him in order to acknowledge his never ceasing interest in this topic and his fundamental contributions to it. We thank Dr. C. Sudfeldt for helpful discussions and S. Wulff for technical assistance with purification of the enzyme.

REFERENCES

Abragam, A., & Bleaney, B. (1970) in *Electron Paramagnetic Resonance of Transition Ions*, Clarendon, Oxford.

Antanaitis, B. C., Brown, R. D., Chasteen, N. D., Freedman, J. H., Koenig, S. H., Lilienthal, H. R., Peisach, J., & Brewer, C. F. (1987) *Biochemistry 26*, 7932−7937.

Bock, K., Meldal, M., Meyer B., & Wiebe, L. (1983) *Acta Scand. Ser. B37*, 101−108.

Bogumil, R., Hüttermann, J., Kappl, R., Stabler, R., Sudfeldt, C., & Witzel, H. (1991) *Eur. J. Biochem. 196*, 305−312.

Bogumil, R., Kappl, R., Hüttermann, J., Sudfeldt, C., & Witzel, H. (1993) *Eur. J. Biochem. 213*, 1185−1192.

Callens, M., Kersters-Hilderson, H., Van Opstal, O., & De Bruyne, C. K. (1986) *Enzyme Microb. Technol. 8*, 696−400.

Callens, M., Tomme, P., Kersters-Hilderson, H., Cornelis, R., Vangrysperre, W., & De Bruyne, C. K. (1988) *Biochem. J. 250*, 285−290.

Carrell, H. L., Rubin, B. H., Hurley, T. J., & Glusker, J. P. (1984) *J. Biol. Chem. 259*, 3230−3236.

Carrell, H. L., Glusker, J. P., Burger, V., Manfre, F., Tritsch, D., & Biellmann, J.-F. (1989) *Proc. Natl. Acad. Sci. U.S.A. 86*, 4440−4444.

Collyer, C. A., Henrick, K., & Blow, D. M. (1990) *J. Mol. Biol. 212*, 211−235.

Dauter, Z., Dauter, M., Hemker, J., Witzel, H., & Wilson, K. S (1989) *FEBS Lett. 247*, 1−8.

Dauter, Z., Terry, H., Witzel, H., & Wilson, K. S. (1990) *Acta Crystallogr. B46*, 833−841.

Dikanov, S. A., Tyryshkin, A. M., Hüttermann, J., Bogumil, R., & Witzel, H. (1995) *J. Am. Chem. Soc. 117*, 4976−4986.

Farber, G. A., Glasfeld, A., Tiraby, G., Ringe, D., & Petsko, G. A. (1989) *Biochemistry 28*, 7289−7297.

Hardman, K. D., Agarwar, R. C., & Freiser, (1982) *J. Mol. Biol. 157*, 69−81.

Henrick, K., Collyer, C. A., & Blow, D. M. (1989) *J. Mol. Biol. 208*, 129−157.

Jenkins, J., Janin, J., Rey, F., Chiadmi, M., van Tilbeurgh, H., Lasters, I., De Maeyer, M., Van Belle, D., Wodak, S. J., Lauwereys, M., Stanssens, P., Mrabet, N. T., Snauwaert, J., Matthyssens, G., & Lambeir, A.-M. (1992) *Biochemistry 31*, 5449−5458.

Kasumi, T., Hayashi, K., & Tsumura, N. (1982) *Agric. Biol. Chem. 46*, 21−30.

Lambeir, A.-M., Lauwereys, M., Stanssens, P., Mrabet, N. T., Snauwaert, J., van Tilbeurgh, H., Matthyssens, G., Lasters, I., De Maeyer, M., Wodak, S. J., Jenkins, J., Chiadmi, M., & Janin, J. (1992) *Biochemistry 31*, 5459−5466.

Lavie, A., Allen, K. I., Petsko, G. A., & Ringe, D. (1994) *Biochemistry 33*, 5469−5480.

Meng, M., Lee, C., Bagdasarian, M., & Zeikus, J. G. (1991) *Proc. Natl. Acad. Sci. U.S.A. 88*, 4015−4019.

Meng, M., Bagdasarian, M., & Zeikus, G. J. (1993) *Proc. Natl. Acad. Sci. U.S.A. 90*, 8459−8463.

Reed, G. H., & Ray, W. R. (1971) *Biochemistry 10*, 3190−3197.

Reed, G. H., & Markham, G. D. (1984) in *Biological Magnetic Resonance* (Berliner, J. L., & Reuben, J., Eds.) Vol. 6, pp 73−142, Plenum Press, New York.

Rey, F., Jenkins, J., Janin, J., Lasters, I., Alard, P., Claessens, M., Matthyssens, G., & Wodak, S. (1988) *Proteins 4*, 165−172.

Sanchez, S., & Smiley, K. L. S. (1975) *Appl. Microbiol. 29*, 745−750.

Schray, K. J., & Rose, I. A. (1971) *Biochemistry 10*, 1058−1062.

Sudfeldt, C., Schäffer, A., Kägi, J., Bogumil, R., Schulz, H.-P., Wulff, S., & Witzel, H. (1990) *Eur. J. Biochem. 193*, 863−881.

Takasaki, Y. (1966) *Agric. Biol. Chem. 30*, 1247−1251.

van Bastelaere, P., Vangrysperre, W., & Kersters-Hilderson, H. (1991) *Biochem. J. 278*, 285−292.

Verhoff, F. H., Bogulawski, G., Lantero, O. J., Schlager, S. T., & Jao, Y. C. (1985) in *Comprehensive Biotechnology* (Balanch, H. W., Drew, S., & Wang, D. I. C., Eds.) Vol. 3, pp 837−885, Pergamon Press, Oxford.

Whitlow, M., Howard, A. J., Finzel, B. C., Poulos, T. L., Winborne, E., & Gilliland, G. L. (1991) *Proteins 9*, 153−173.

Wieghardt, K. (1989) *Angew. Chem. 101*, 1179−1198.

BI962406N